Equilibrium-Aware Shape Design for Concrete Printing

Shajay Bhooshan(✉), Tom Van Mele, and Philippe Block

ETH Zurich, Institute of Technology in Architecture, Block Research Group, Stefano-Franscini-Platz 5, HIL H 46.2, 8093 Zurich, Switzerland
bhooshan@arch.ethz.ch

Abstract. This paper proposes an Interactive Design Environment and outlines the underlying computational framework to adapt equilibrium modelling techniques from rigid-block masonry to the multi-phase material typically used in large-scale additive manufacture. It focuses on enabling the synthesis of geometries that are structurally and materially feasible vis-a-vis 3D printing with compression-dominant materials. The premise of the proposed research is that the material printed in layers can be viewed as micro-scale bricks that are initially soft, and harden over time—a kind of micro-stereotomy. This insight, and the observation about the necessity of design exploration yields the principal contributions of the paper: A computational framework that allows for geometric reasoning about shape and exploration of associated design-space, and early, proof-of-concept results.

Keywords: 3D printing · Equilibrium modelling · Shape design · Unreinforced masonry · Concrete and clay printing

Motivation

The shape-design and computational framework that is outlined in this paper is motivated by the rapid growth in desktop and large scale 3D printing and the lack of exploratory design tools thereof. The framework is based on a novel insight regarding the applicability of design and analysis methods used in unreinforced masonry to large scale, layered 3D printing with compression dominant materials such as concrete and clay.

Large Scale 3D Printing and Lack of Tools for Design Exploration

Khoshnevis et al. (2006) of Contour-crafting®, pioneers in large-scale 3D printing, deliberate two particular, shape-design related working points for the further development of the technology: (1) expressiveness of geometric modelling for designers and (2) constructive guidance about the feasibility constraints imposed by the fabrication process. Similar design and data related issues were also outlined and nominally addressed, by the other pioneering effort at Loughborough University (Buswell et al. 2008). Further, necessity and opportunity for exploring the very design related aspects that have hitherto been side-lined, is highlighted in the maturation of the concrete

K. De Rycke et al., *Humanizing Digital Reality*,
https://doi.org/10.1007/978-981-10-6611-5_42

printing technology in the last decade, along with the advent of several new competitors (Khoshnevis 2004; Buswell et al. 2007; Dini 2009; CyBe-Construction 2016; XtreeE 2016).

Compatibility of Funicular Structures and Concrete Printing

The dominant structural properties of printed concrete are high density ($\sim$2.2 Tons/m^3), high compressive strength ($\sim$100 MPa), relative weak flexural strength (10% of compressive strength), and a unique orthotropic behaviour induced by the layered printing process, yielding a weak tensile bond between layers ($\sim$0.5–3 MPa) (Le et al. 2012a; Perrot et al. 2016; Wangler et al. 2016) (Fig. 1). These properties make it well suited for the adaptation of the design methods of unreinforced masonry structures, including the historic methods of graphics statics (Culmann 1875), their application to the design of concrete structures (Zastavni 2008; Fivet and Zastavni 2012), and their recent computational extensions (Block and Ochsendorf 2007; De Goes et al. 2013; Vouga et al. 2012; Tang et al. 2012; Liu et al. 2013; Van Mele et al. 2014). In addition, the structural aspects of the practice of stereotomy (Sakarovitch 2003; Fallacara 2009; Rippmann 2016), which align material layout with expected force flow through the structure, are particularly relevant. The layered filaments of concrete printing, especially when they can be aligned along orthonormal directions of a surface (Gosselin et al. 2016), would require similar careful alignment. The premise of the proposed research is that the material printed in layers can be viewed as micro-scale bricks that are initially soft, and harden into rigid filaments (blocks) over time—a kind of micro-stereotomy (Fig. 1 right).

Objectives and Contributions

The primary objective of the research presented, is the synthesis of geometries that are structurally and materially feasible vis-a-vis 3D printing with compression-dominant materials. In other words, equilibrium aware, shape-design for concrete printing.

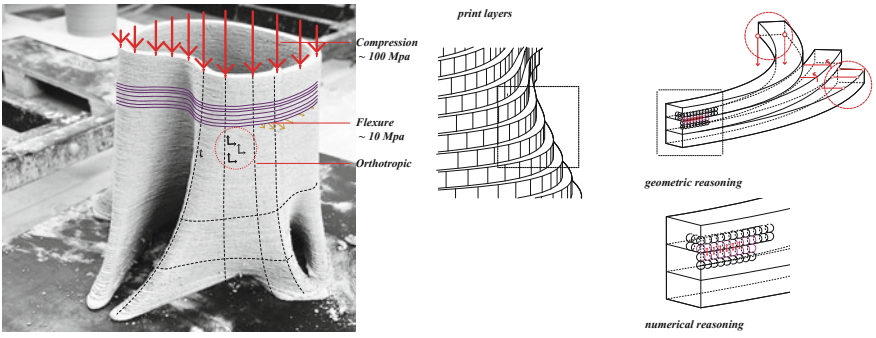

Fig. 1. *Left* dominant material properties of printed concrete. *Right* intention to discretise the print layers into micro-blocks, to enable geometric reasoning about equilibrium and print feasibility

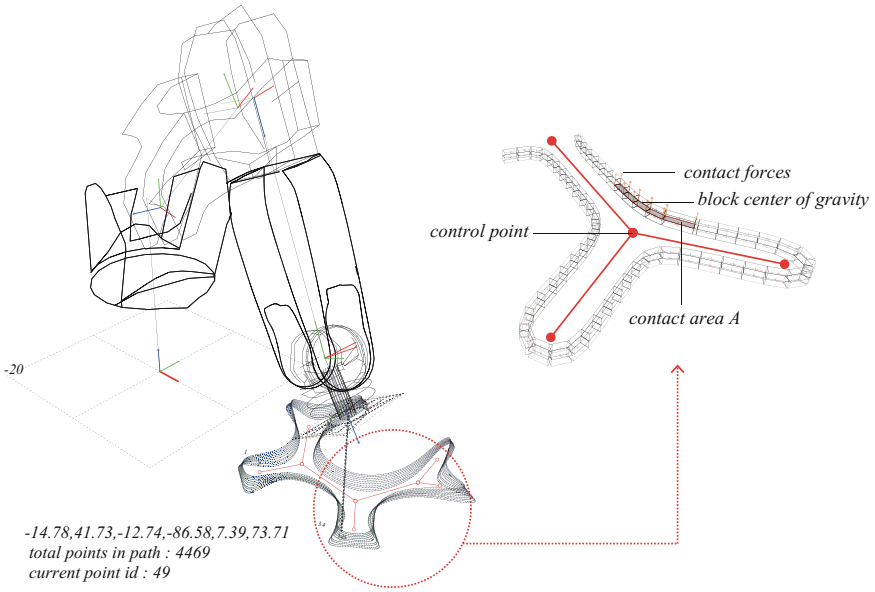

Fig. 2. Interactive design explorer (IDE) for concrete printing

The insight relating unreinforced masonry to 3D Printing and the preceding observation about the necessity of design exploration for the further development of 3D printing as an architectural tool yields the principal contributions of the paper: A computational framework that allows for a geometric reasoning about shape and exploration of the associated design-space of novel and feasible shapes. As a specific contribution, the proposed Interactive Design Environment (IDE) (Fig. 2) and the underlying computational framework (CF) adapt equilibrium modelling techniques from rigid-block masonry to the multi-phase material typically used in large-scale additive manufacturing. Lastly, proof-of-concept physical outcomes are an additional contribution.

Related Work

Design Paradigm Aspects

The importance of geometric methods of structural design, and the benefits of integrating structural and construction-aware computational methods in the early-design phase is well argued in Lachauer (2015) and Rippmann (2016). Recent developments in the field of Architectural Geometry, with its explicit aim of "incorporation of essential aspects of function, fabrication and statics into the shape modelling process" (Jiang et al. 2015), extend this so-called Computer Aided Geometric Design (CAGD) paradigm to architectural design. In the realm of large-scale 3D printing however, these

design aspects have not received much attention, barring a few recent efforts (De Kestelier and Buswell 2009; Chien et al. 2016; Wolfs and Salet 2015).

Computational Aspects

Computational modelling of 3D printing should consider both structural stability of complex geometries made of printed concrete and the feasibility of printing them (Fig. 3). The first is a problem of developing geometries aligned with expected loading and force-flow. The second is additionally, dependent on time, material rheology etc. Materially, the hardened state of the concrete can be considered orthotropic (Fig. 1) and the fresh state is often considered a so-called visco-plastic Bingham material (Mechtcherine et al. 2014; Tanigawa and Mori 1989).

Equilibrium of Soft-Rigid Material

The proposed computational framework (CF) intends to unify the representation of both the aspects above. The idea here is to scale-down and adapt equilibrium modelling methods based on rigid-body mechanics, to include semi-rigid and time-dependent behaviour. Thus the two classes of methods that encode rigid-body mechanics—rigid-body dynamics (RBD) and rigid-block equilibrium (RBE)—are important precedents. The research presented here is based on the established methods of RBD (Hahn 1988; Baraff 1989; Hart et al. 1988) and RBE (Livesley 1978; Whiting 2012; Heyman 1966; Livesley 1992). Specifically, the proposed method extends the RBE method of Frick et al. (2015) to accommodate the soft-rigid aspects of 3D printing of concrete.

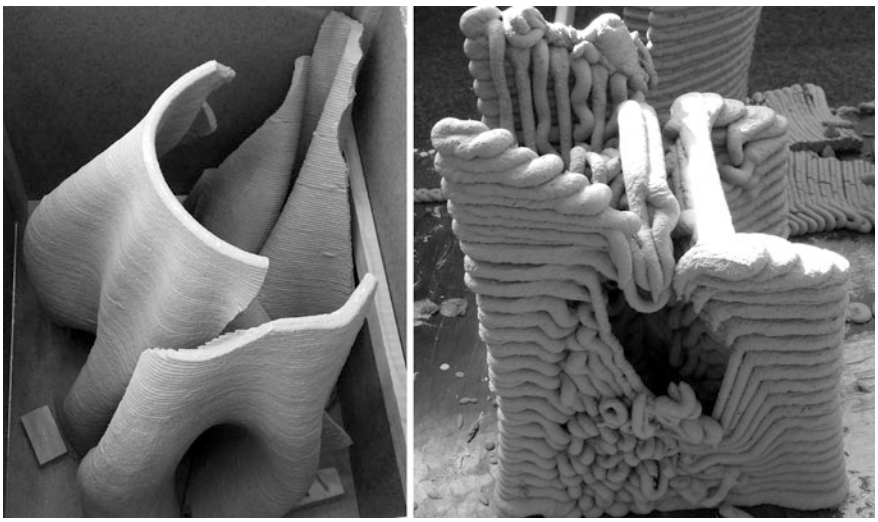

Fig. 3. Two particular phenomena to be addressed: stability of the printed shapes (*left*) and the feasibility of printing them (*right*)

It can be noted that several other state-of-the-art methods were considered including the ubiquitous Finite Element Method (Tanigawa and Mori 1989; Kwon 2002), Material-point methods (Sulsky et al. 1995; Stomakhin et al. 2013), and Discrete Element Methods (Cundall and Strack 1979; Harada 2007; Shyshko and Mechtcherine 2008). The reasons for the choice stem from the motivations mentioned previously: operating in the CAGD paradigm and therefore, extending methods that use geometry-based approaches to solve the equilibrium problem.

Computational Framework

The proposed research considers design of geometries for concrete printing as micro-stereotomy, where the micro-scale material layout is a function of structural and fabrication constraints. Further, the objective of the proposed computational framework (CF) is to directly and procedurally generate the trajectories of the print head of the 3D Printer—the so-called task graphs (Khoshnevis et al. 2006)—utilizing the various degrees of freedom of the printer, whilst ensuring stability of the printed shape and its print feasibility. These two aspects represent the principal components of the IDE (Fig. 4) and are outlined next.

Synthesis of Task Graphs

Task graphs can be produced by processing either explicit, mesh representations (Fig. 5 left and middle) or implicit, distance field representations of geometry. The proposed method for procedural, force-aligned stereotomy is to utilise the latter. In other words, task graphs are a function of the level curves of user-defined scalar functions (Fig. 6). Thus, the IDE helps design appropriate scalar functions, whose contours represent task graphs. This is expanded in Sect. 4.

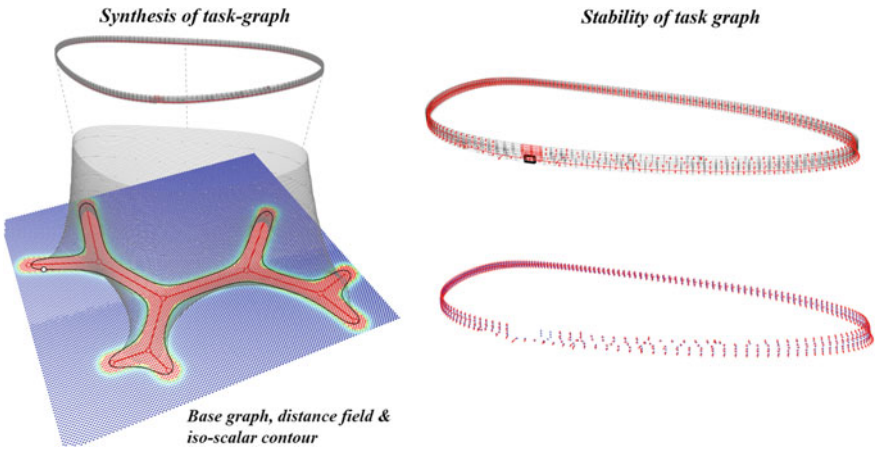

Fig. 4. Synthesis of task graphs from scalar fields (*right*), and the evaluation of their static equilibrium (*left*)

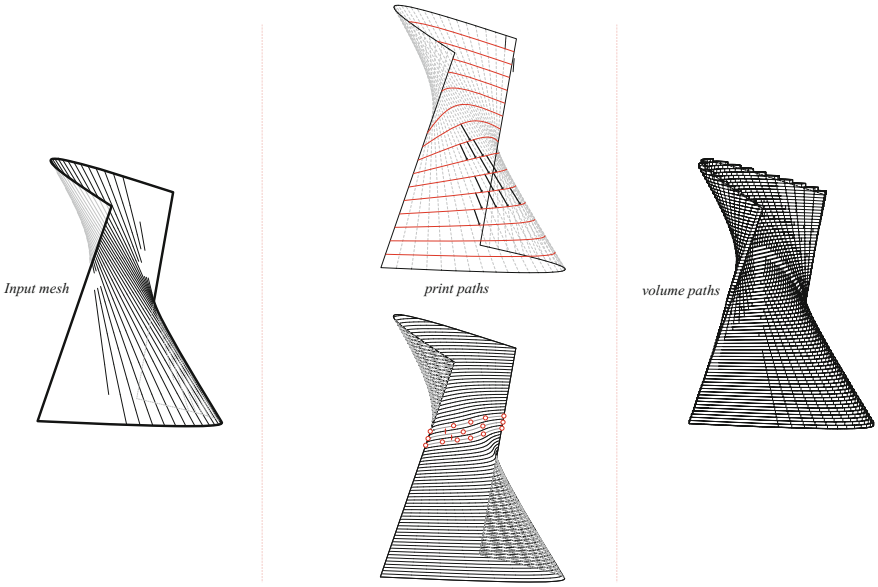

Fig. 5. Processing of mesh representation (*left*) to generate horizontal or field-aligned task graphs (*middle*) and subsequent attaching of a micro-block model to evaluate their stability (*right*)

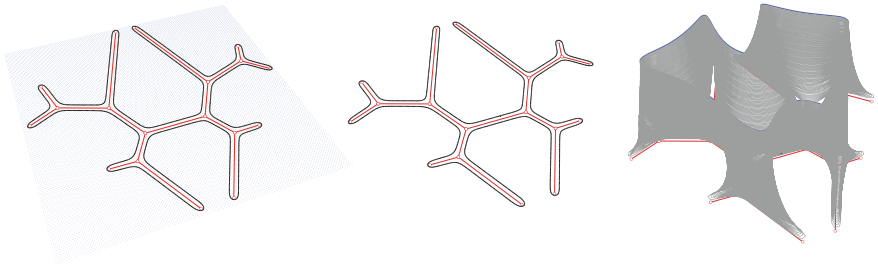

Fig. 6. (*Left*) a user-specified skeleton graphs (*red*) and related distance field. (*Middle*) Extracted level curve. (*Right*) 2.5D evolution of level curve (*blue*) and resulting task graphs

Stability of Task Graphs

The task graphs, once extracted from either implicit or explicit representations, are populated with micro-scale blocks (Fig. 5 right). These blocks are needed in evaluating the task graphs for their structural and material feasibility using the proposed static equilibrium model, as described in Sect. 5.

Procedural Shape Design

To aid the user-controlled synthesis of the task graphs, the IDE utilises a combination of implicit scalar field representation and resulting level curves as the data structure to represent the geometries to be printed. Additionally, the level curve can be evolved as it is extruded in the z-direction, resulting in a so-called 2.5D extrusion (Fig. 6 right). A skeletal graph is employed to manipulate the scalar field and thus the resulting task graphs (Fig. 6 middle). In combination, it bears similarity to the so-called skeleton-mesh co-representation (SMC) used in popular digital sculpting software such as Autodesk MudBox™ and Pixelogic ZBrush™ (Ji et al. 2010; Bærentzen et al. 2014). The choice for this data structure is a consequent of the design and fabrication related aspects outlined below.

A Forward Approach to Synthesize Feasible Geometries

A common method to produce materially feasible geometries is to start with a reasonable guess of such geometry and perturb it to a near-by state that satisfies structural and fabrication constraints. Such a process could be termed as the *inverse* approach to *modelling* of geometry. For a summary of the vast amount of methods and literature available in mesh segmentation and other techniques of stereotomic design, the reader is referred Sect. 6.3 of Rippmann (2016). Conversely, a *forward* approach aims to procedurally synthesize geometries that satisfy the same constraints. The likelihood of discovering novel shapes and possibilities is higher with the forward approach and this is an important motivation as previously mentioned.

Fabrication Constraints

Discretisation of geometry into layers and layers further into micro-blocks must allow for the newest layer of material to remain accessible to the print head. This is achieved by formulating the scalar field representation as a distance field defined in relation to the skeleton graph. In other words, the skeletal graph is in fact the medial axis of the scalar field, and medial axis guarantees the outward radiating property (Fig. 7). Further, it would be beneficial to align the print layers in orthonormal directions to the expected force flow. Level curves of scalar fields naturally achieve this.

Interactivity

To keep with the edit-and-observe contemporary paradigm of CAGD, it is important to provide appropriate, non-numeric methods of user-control of the critical geometric parameters of the computational model (Fig. 8).

Static Equilibrium Model

As mentioned previously, this second aspect of the IDE, extends the RBE method to accommodate the soft-rigid aspects of 3D printing of concrete.

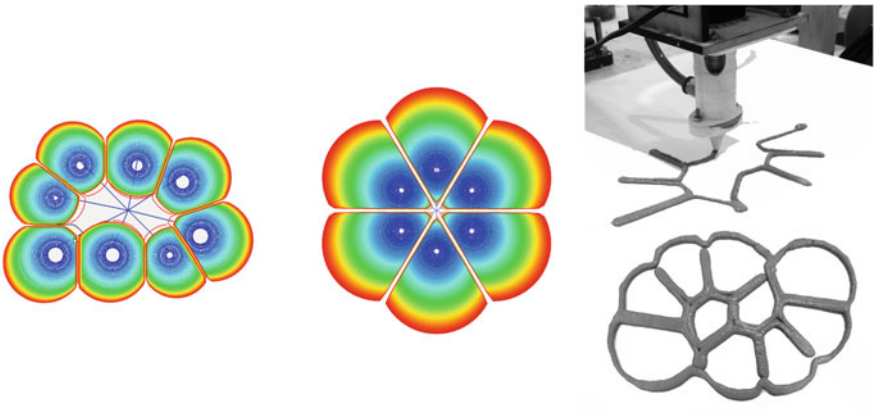

Fig. 7. Outward radiating task graph as a result of a radial distance function

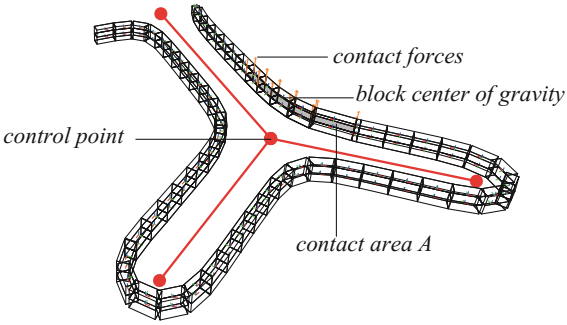

Fig. 8. A user-specified skeletal graphs and a micro-block model attached to the resulting task graph. The intermediate representation of the level curve/task graph is hidden in this case. The skeletal graph serves as a manipulator whilst satisfying fabrication constraints

Rigid-Block Equilibrium

Popular implementations of RBE and RBD mentioned previously, share a common mathematical formulation: computations at a single time instance of RBD calculates the linear and angular accelerations of each block, whilst RBE inverse computes the forces and torques on each block by setting their accelerations to zero. Further, the two algorithms converge to be exactly the same when RBD computes the so-called *resting contact* forces—forces needed to keep two static rigid bodies from inter-penetrating (Baraff 1997). In this case, both algorithms find the necessary equilibrating forces (shown in orange in Fig. 9) that satisfy linear constraints using quadratic programming.

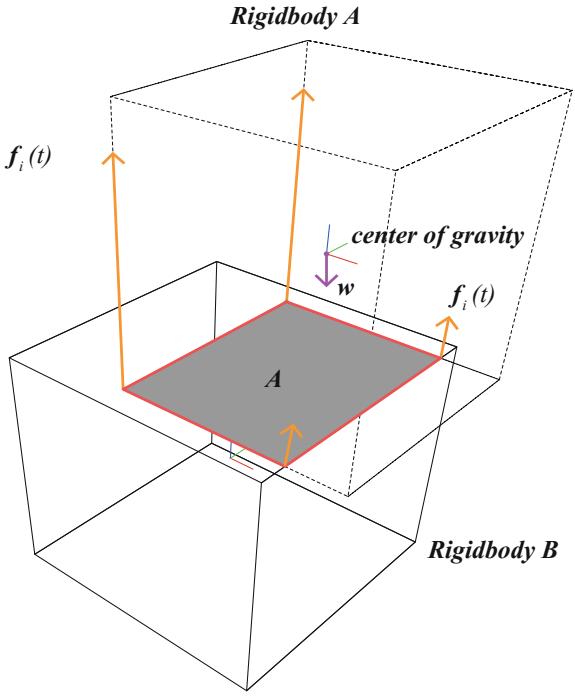

Fig. 9. Contact interface and forces when two rigid-bodies are in resting contact

Equilibrium Formulation

The formulation for resting contact forces in RBD (Baraff 1997) (Fig. 9) is

$$\boldsymbol{A}_{\text{eq}}\boldsymbol{f} + \boldsymbol{b} = \boldsymbol{a} \tag{1}$$

where $\boldsymbol{a}$ is a column vector that encodes accelerations of the blocks, $\boldsymbol{A}_{\text{eq}}$ is the so-called $n \times n$ equilibrium matrix, $\boldsymbol{b}$ is a column of constants, $\boldsymbol{f}$ a column vector of unknown force magnitudes, and n is the number of vertices in the contact interface.

When computing *resting contact* forces, $\boldsymbol{b}$ is a column vector of weights of the rigid blocks, $\boldsymbol{a}$ is 0. Thus (1) becomes,

$$\boldsymbol{A}_{\text{eq}}\boldsymbol{f} + \boldsymbol{w} = 0 \tag{2}$$

This is the equilibrium formulation used in RBE to solve for $\boldsymbol{f}$ in a least-squares sense

$$\begin{aligned} &\min g(\boldsymbol{f}) = \boldsymbol{f}^T\boldsymbol{H}\boldsymbol{f} + \boldsymbol{b}^T \\ &s.t \quad A_{\text{eq}}\boldsymbol{f} + \boldsymbol{w} = 0 \end{aligned} \tag{3}$$

For derivation, detailed explanation and pseudo code, see (Livesley 1978; Frick et al. 2015; Baraff 1997).

Soft-Rigid Body Equilibrium (SRBE)

The proposed CF extends the RBE method above, to semi-rigid and rigidifying materials such as fresh concrete and clay. The insight here is that, the necessary forces at the contact interface, $\boldsymbol{f}_i(t)$ and highlighted orange in Fig. 10, that ensure static equilibrium of the rigidified blocks is a function of the configuration of the blocks. On the other hand, the capacity of the rigidifying material to be able to offer the necessary reaction forces $\boldsymbol{g}_i(t)$ (highlighted green in Fig. 10), are a function of time. In other words, the time-dependent reaction forces (Wangler et al. 2016; Le et al. 2012b) can be added as an additional constraint to the quadratic program (3) that computes the equilibrating forces.

Implementation

The current implementation of the CF shown in Fig. 11, utilises extensions to the RBE method as stated in Frick et al. (2015), and resting contact formulations and quadratic programming (QP) as stated in Baraff (1997). The ALGLIB library is used to numerically solve the QP.

Contact Interfaces and Collisions

In order to compute the forces or accelerations, both RBD and RBE methods require efficient routines to calculate the so-called contact interface between two colliding or

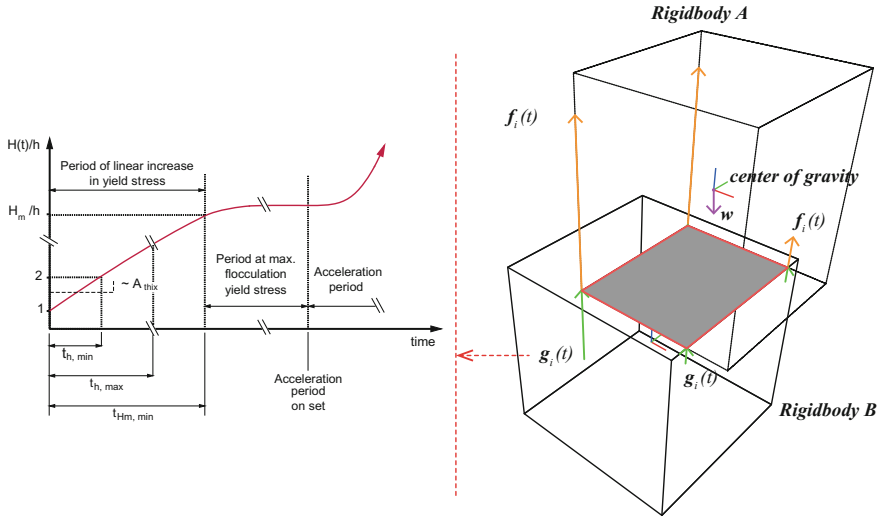

Fig. 10. Soft-rigid body equilibrium forces (*right*) and (*left*) time-dependent evolution of the bearing capacity of the material. Graph from Wangler et al. (2016)

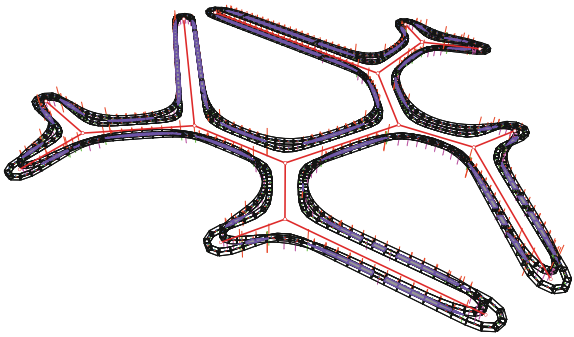

Fig. 11. Application of method to test print feasibility. In the current implementation, areas where a non-trivial contact (*blue*) interface exists, the sRBE method is executed to evaluate feasibility. If such contact is not found, the infeasibility is indicated by *pink arrows*. The skeletal graph (*red*) is manipulated based on this visual feedback

touching rigid bodies (Cundall 1988; Frick et al. 2016). This paper implements only the *face-to-face* contact interface as described in Frick et al. (2016), since it was found to be sufficient to provide interactive feedback to designers. The other interfaces including *face-edge*, are likely to be a result of un-printable geometry.

Results

The synthesized and evaluated task graphs are subsequently processed for printer related parameters such as accessibility of the print-head, speed etc (Fig. 12). The exported print-file is subsequently processed by the manufacturer for additional parameters before being printed (Fig. 13).

The 3D printed outcomes of the shapes designed using the proposed IDE, demonstrate areas of local overhang and under-cuts (Figs. 13 right and 14 left and middle). The overall stability of the prints and their feasibility were able to be reasoned geometrically as exemplified by the inverted printing direction of the shape shown in Fig. 13. The results also demonstrate the usefulness of the 2.5D extrusion method to generate shapes of considerable complexity, which can nonetheless be controlled with nominal parameters. Furthermore, the potential exploitation of non-horizontal print layers is also indicated (Fig. 14 right) and is discussed next.

Discussion and Future Work

The early exploratory design outcomes and physical realisations also demonstrate the potential avenues for refinement and extension of the proposed method. Significant of these are discussed below.

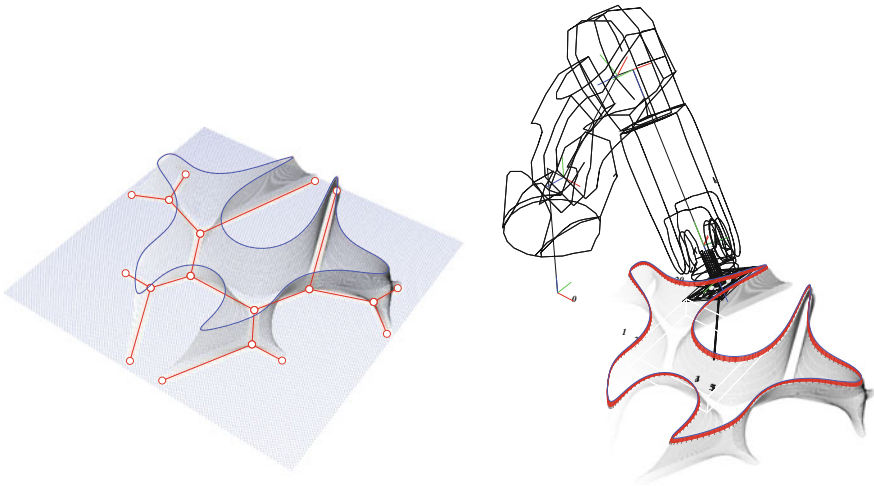

Fig. 12. Post-processing of task graphs for printed related parameters within the IDE

Fig. 13. *Left* processing of an outcome produced by proposed IDE by the manufacturer. *Right* prototype demonstrating the application of the proposed method. Printed at the RexLab, Institute of Experimental Architecture, at Innsbruck. Images courtesy Johannes Ladinig

Fig. 14. (*Left* and *Middle*) Results from the 2.5D extrusion. (*Right*) Non-horizontal extrusion. Printed at the RexLab, Institute of Experimental Architecture, at Innsbruck. Images courtesy Johannes Ladinig

Extension to 3D

The proposed 2.5D synthesis method can be extended to fully 3D spatial skeletons (Figs. 15 and 14 right) as seen in the work of Antonio Gaudi, particularly in the *Sagrada Familia* (Hernandez 2006; Monreal 2012). However, this involves the non-trivial aspect of processing of nodes (Fig. 15 middle) including assigning an appropriate print direction to the nodes, the relative sizes of the edges and nodes (Fig. 15 right) and assigning a sequence for printing. This is currently being implemented.

Exploration of Design Space and Unification of Synthesis and Evaluation

The current linear work-flow between the two main design aspects—synthesis and evaluation, and the subsequent evaluation of the printer-related parameters is already proving useful in exploring the design-space of structurally and materially feasible geometries (Figs. 14 and 16). The unification of the structural and printer-related

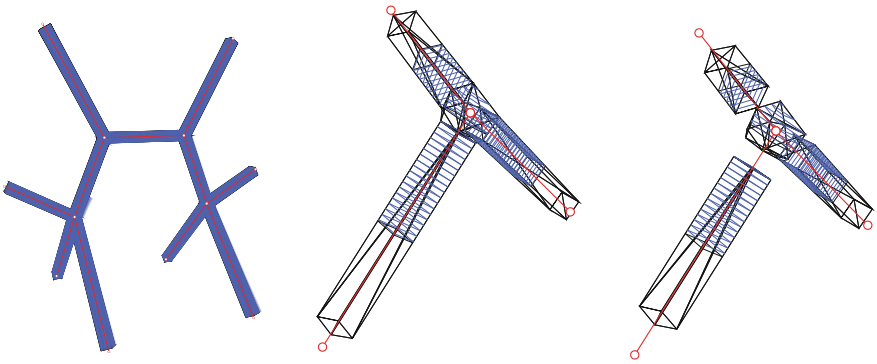

Fig. 15. Extending the 2.5D evolution to multiple, non-vertical, normal directions

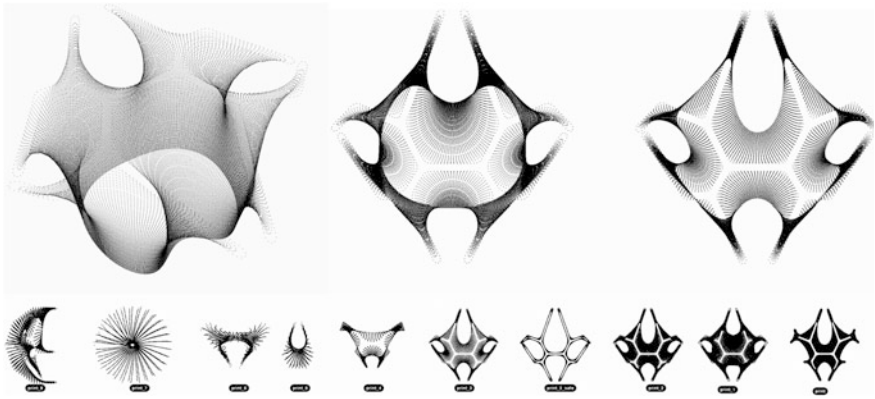

Fig. 16. Exploration of structurally and materially feasible design-space

parameters as constraints within the synthesis of the task graphs will be beneficial to fully support the contemporary edit-and-observe design paradigm, as also for the automated exploration of the parameter-space.

Extension to Other Materials

The proposed sRBE method, given its foundations in design methods for unreinforced rigid-block masonry, could allow for its use in masonry applications that require the modelling of mortar. Current RBE methods do not fully take into account presence of mortar. Since the time-dependent properties of rigidifying materials are encapsulated within a graph, the sRBE method could potentially be extended to other materials that can similarly be encoded—clay, certain food materials such as chocolate and pasta etc.

Conclusions

An Interactive Design Environment (IDE) for the shape design and production of clay printing was outlined, along with an underlying computational framework. Early proof-of-concept physical outcomes were also shown. The novel insight of extending methods from design and analysis of unreinforced masonry to large-scale 3D printing and the proposed computational framework bears promise in the aspects listed below. It can be remembered that these were previously earmarked to be addressed (Khoshnevis et al. 2006) but had hitherto been side-lined:

- abstraction of numerical analysis of feasibility into geometric reasoning,
- developing of an atlas of feasible and novel geometries,
- the applicability of historic techniques of masonry construction and construction, to layered printing,
- data structures amenable to interactive design exploration and
- unifying the equilibrium of printed geometries, along with the print feasibility of the parts.

All aspects mentioned above, though showing promise, require further careful design of data structures, mathematical formulations, and algorithms to fully realise the objectives.

References

Bærentzen, J.A., Abdrashitov, R., Singh, K.: Interactive shape modeling using a skeleton-mesh co-representation. ACM Trans. Graph. (TOG) **33**(4), 132 (2014)

Baraff, D.: Analytical methods for dynamic simulation of non-penetrating rigid bodies. In: ACM SIGGRAPH Computer Graphics, pp. 223–232. ACM (1989)

Baraff, D.: An introduction to physically based modeling: rigid body simulation II—nonpenetration constraints. In: SIGGRAPH Course Notes, pp. D31–D68 (1997)

Block, P., Ochsendorf, J.: Thrust network analysis: a new methodology for three-dimensional equilibrium. J. Int. Assoc. Shell Spat. Struct. **155**, 167 (2007)

Buswell, R.A., et al.: Freeform construction: mega-scale rapid manufacturing for construction. Autom. Constr. **16**(2), 224–231 (2007)

Buswell, R.A., et al.: Design, data and process issues for mega-scale rapid manufacturing machines used for construction. Autom. Constr. **17**(8), 923–929 (2008)

Chien, S., et al.: Parametric customisation of a 3D concrete printed pavilion. In: Proceedings of the 21st International Conference of the Association for Computer-Aided Architectural Design Research in Asia CAADRIA 2016, pp. 549–558. The Association for Computer-Aided Architectural Design Research in Asia (CAADRIA), Hong Kong (2016)

Culmann, K.: Die graphische statik. Meyer & Zeller (A. Reimann), Zurich (1875)

Cundall, P.A.: Formulation of a three-dimensional distinct element model—part I. A scheme to detect and represent contacts in a system composed of many polyhedral blocks. In: International Journal of Rock Mechanics and Mining Sciences & Geomechanics Abstracts, pp. 107–116. Elsevier (1988)

Cundall, P.A., Strack, O.D.L.: A discrete numerical model for granular assemblies. Geotechnique **29**(1), 47–65 (1979)

CyBe-Construction: CyBe Construction—Redefining Construction. Available at: https://www.cybe.eu/ (2016)

De Goes, F., et al.: On the equilibrium of simplicial masonry structures. ACM Trans. Graph. (TOG) **32**(4), 93 (2013)

De Kestelier, X., Buswell, R.A.: A digital design environment for large-scale rapid manufacturing. In: Proceedings of the 29th Annual Conference of the Association for Computer Aided Design in Architecture, pp. 201–208 (2009)

Dini, E.: D-Shape. Monolite UK Ltd. http://www.d-shape.com/cose.htm (2009)

Fallacara, G.: Toward a stereotomic design: experimental constructions and didactic experiences. In: Proceedings of the Third International Congress on Construction History, p. 553 (2009)

Fivet, C., Zastavni, D.: Robert Maillart's key methods from the Salginatobel Bridge design process (1928). J. Int. Assoc. Shell Spat. Struct. J. IASS **53**(171), 39–47 (2012)

Frick, U., Van Mele, T., Block, P.: Data management and modelling of complex interfaces in imperfect discrete-element assemblies. In: Proceedings of the International Association for Shell and Spatial Structures (IASS) Symposium, Tokyo, Japan (2016)

Frick, U., Van Mele, T., Block, P.: Decomposing three-dimensional shapes into self-supporting, discrete-element assemblies. In: Modelling Behaviour, pp. 187–201. Springer (2015)

Gosselin, C., et al.: Large-scale 3D printing of ultra-high performance concrete—a new processing route for architects and builders. Mater. Des. **100**, 102–109 (2016)

Hahn, J.K.: Realistic animation of rigid bodies. In: ACM SIGGRAPH Computer Graphics, pp. 299–308. ACM (1988)

Harada, T.: Real-time rigid body simulation on GPUs. GPU Gems **3**, 123–148 (2007)

Hart, R., Cundall, P.A., Lemos, J.: Formulation of a three-dimensional distinct element model—part II. Mechanical calculations for motion and interaction of a system composed of many polyhedral blocks. In: International Journal of Rock Mechanics and Mining Sciences & Geomechanics Abstracts, pp. 117–125. Elsevier (1988)

Hernandez, C.R.B.: Thinking parametric design: introducing parametric Gaudi. Des. Stud. **27**(3), 309–324 (2006)

Heyman, J.: The stone skeleton. Int. J. Solids Struct. **2**(2), 249–279 (1966)

Ji, Z., Liu, L., Wang, Y.: B-Mesh: a modeling system for base meshes of 3D articulated shapes. In: Computer Graphics Forum, pp. 2169–2177. Wiley Online Library (2010)

Jiang, C., et al.: Interactive modeling of architectural freeform structures: combining geometry with fabrication and statics. In: Advances in Architectural Geometry 2014, pp. 95–108. Springer (2015)

Khoshnevis, B.: Automated construction by contour crafting—related robotics and information technologies. Autom. Constr. **13**(1), 5–19 (2004)
Khoshnevis, B., et al.: Mega-scale fabrication by contour crafting. Int. J. Ind. Syst. Eng. **1**(3), 301–320 (2006)
Kwon, H.: Experimentation and analysis of contour crafting (CC) process using uncured ceramic materials, thesis, University of Southern California, California (2002)
Lachauer, L.: Interactive Equilibrium Modelling—A New Approach to the Computer-Aided Exploration of Structures in Architecture. Ph.D. thesis. ETH Zurich, Department of Architecture, Zurich (2015)
Le, T.T., Austin, S.A., Lim, S., Buswell, R.A., Law, R., et al.: Hardened properties of high-performance printing concrete. Cem. Concr. Res. **42**(3), 558–566 (2012a)
Le, T.T., Austin, S.A., Lim, S., Buswell, R.A., Gibb, A.G.F., et al.: Mix design and fresh properties for high-performance printing concrete. Mater. Struct. **45**(8), 1221–1232 (2012b)
Liu, Y., et al.: Computing self-supporting surfaces by regular triangulation. ACM Trans. Graph. (TOG) **32**(4), 92 (2013)
Livesley, R.K.: Limit analysis of structures formed from rigid blocks. Int. J. Numer. Methods Eng. **12**(12), 1853–1871 (1978)
Livesley, R.K.: A computational model for the limit analysis of three-dimensional masonry structures. Meccanica **27**(3), 161–172 (1992)
Mechtcherine, V., et al.: Simulation of fresh concrete flow using Discrete Element Method (DEM): theory and applications. Mater. Struct. **47**(4), 615–630 (2014)
Monreal, A.: T-norms, T-conorms, aggregation operators and Gaudí's columns. In: Soft Computing in Humanities and Social Sciences, pp. 497–515. Springer (2012)
Perrot, A., Rangeard, D., Pierre, A.: Structural built-up of cement-based materials used for 3D-printing extrusion techniques. Mater. Struct. **49**(4), 1213–1220 (2016)
Rippmann, M.: Funicular Shell Design: Geometric Approaches to Form Finding and Fabrication of Discrete Funicular Structures. Ph.D. Thesis, ETH Zurich, Department of Architecture, Zurich (2016)
Sakarovitch, J.: Stereotomy, a multifaceted technique. In: Huerta, S. (ed.) Proceedings of the 1st International Congress on Construction History, Madrid, pp. 69–79 (2003)
Shyshko, S., Mechtcherine, V.: Simulating the workability of fresh concrete. In: Proceedings of the International RILEM Symposium Of Concrete Modelling—CONMOD, pp. 173–181 (2008)
Stomakhin, A., et al.: A material point method for snow simulation. ACM Trans. Graph. (TOG) **32**(4), 102 (2013)
Sulsky, D., Zhou, S.-J., Schreyer, H.L.: Application of a particle-in-cell method to solid mechanics. Comput. Phys. Commun. **87**(1), 236–252 (1995)
Tang, C., et al.: Form-Finding with Polyhedral Meshes Made Simple. http://www.geometrie.tugraz.at/wallner/formfinding2.pdf (2012)
Tanigawa, Y., Mori, H.: Analytical study on deformation of fresh concrete. J. Eng. Mech. **115**(3), 493–508 (1989)
Van Mele, T., et al.: Best-fit thrust network analysis. In: Shell Structures for Architecture-Form Finding and Optimization, pp. 157–170. Routledge (2014)
Vouga, E., et al.: Design of self-supporting surfaces. ACM Trans. Graph. **31**(4) (2012)
Wangler, T., et al.: Digital concrete: opportunities and challenges. RILEM Tech. Lett. **1**, 67–75 (2016)
Whiting, E.J.W.: Design of structurally-sound masonry buildings using 3D static analysis, Diss, Massachusetts Institute of Technology (2012)
Wolfs, R., Salet, T.A.M.: 3D printing of concrete structures, graduation thesis, Technische Universiteit Eindhoven (2015)
XtreeE: XtreeE| The large-scale 3D (2016)
Zastavni, D.: The structural design of Maillart's Chiasso Shed (1924): a graphic procedure. Struct. Eng. Int. **18**(3), 247–252 (2008)